sibly also pertinent to ^{3}He systems in restricted geometries like the registered phase of ^{3}He on Grafoil or the special 2D layers near a liquid-solid interface. Finally it is important to appreciate that the speculation made in this Letter is subject to several caveats[18] that will be present until an exhaustive treatment of 2D vacancy-induced ferromagnetism is complete.

This work was supported in part by the National Science Foundation.

[1]J. G. Dash, *Films on Solid Surfaces* (Academic, New York, 1975).

[2]The behavior of low-coverage helium on Vycor glass or on Mylar is very different from its behavior on Grafoil.

[3]M. Bretz, J. G. Dash, H. C. Hickernell, E. O. McLean, and O. E. Vilches, Phys. Rev. A 8, 1589 (1973).

[4]R. L. Elgin and D. L. Goodstein, Phys. Rev. A 9, 2657 (1974).

[5]B. P. Cowan, M. G. Richards, A. L. Thomson, and W. J. Mullin, Phys. Rev. Lett. 38, 165 (1977); B. P. Cowan, thesis, Sussex University, 1976 (unpublished); R. J. Rollefson, Phys. Rev. Lett. 29, 410 (1972).

[6]M. G. Richards, private communication.

[7]Coverages are given in particles/Å^2.

[8]The signature of melting is seen in specific-heat and NMR data (see Refs. 1 and 5) although the phase diagram may not be as simple for the low-density solids as implied here; see S. V. Hering, S. W. Van Sciver, and O. E. Vilches, J. Low Temp. Phys. 25, 793 (1976).

[9]D. C. Hickernell, E. O. McLean, and O. E. Vilches, J. Low Temp. Phys. 23, 143 (1976).

[10]See, for example, R. A. Guyer, in *Solid State Physics*, edited by H. Ehrenreich, F. Seitz, and D. Turnbull (Academic, New York, 1969), Vol. 23, p. 402.

[11]The idea of "frozen-in" vacancies in bulk helium systems is associated with the discussion of superfluid solids; see R. A. Guyer, J. Low Temp. Phys. 8, 427 (1972).

[12]Guyer, Ref. 11.

[13]Y. Nagaoka, Solid State Commun. 3, 409 (1965).

[14]W. F. Brinkman and T. M. Rice, Phys. Rev. B 2, 1324 (1970).

[15]R. A. Guyer, to be published. This formula is an analytic fit to the band edge of a simple cubic system determined from a study of ten moments. Although the formula is for a simple cubic system it has the qualitative elements that are present for all systems.

[16]J. Sokloff and A. Widom, Phys. Rev. Lett. 35, 673 (1975), and Phys. Rev. B 14, 1146 (1976).

[17]A. I. Ahonen *et al.*, to be published.

[18]For example, Nagaoka's discussion of magnetic ground states depends on geometry and quite possibly on the sign of t and has not been extended to the triangular lattice; the proof by N. D. Mermin and H. Wagner [Phys. Rev. Lett. 17, 1133 (1966)], although not strictly relevant to two-dimensional Grafoil platelets, places limitations on the quantitative deductions of a mean-field calculation.

Phonon Dispersion in Transition Metals

C. M. Varma and W. Weber[(a)]

Bell Laboratories, Murray Hill, New Jersey 07974

(Received 25 August 1977)

We present a new formulation of lattice dynamics especially suitable for transition metals and their compounds. Calculations of the phonon dispersion in $4d$ bcc metals and alloys based on it reproduce all the observed anomalous structure and elucidate the physical origin of the anomalies.

The study of the lattice dynamics of transition metals and compounds (TMC) has been very actively pursued recently.[1-3] Partly the impetus has been generated by the empirical correlation between high superconducting temperatures and the presence of anomalies in the phonon spectra. Microscopic lattice-dynamical calculations for TMC are very complicated when based on the customary method,[4] developed originally for nearly free-electron metals. In this Letter, we present a simple alternative approach and use it to calculate phonon dispersion curves for Nb, Mo, and Nb-Mo alloys. Our results reproduce all anomalous features in the phonon spectra of these materials and allow an understanding of their origin.

In the adiabatic approximation, the phonon frequencies are obtained by diagonalizing the dynamical matrix

$$D_{i\alpha,j\beta} = \nabla_{i\alpha}\nabla_{j\beta}(V_{cc}+E_e). \quad (1)$$

Here i and j are the lattice sites, α and β the Cartesian indices; V_{cc} is the bare ion-ion Coulomb interaction; and the total electronic energy, E_e, is a parametric function of the ionic coordinates.

In the self-consistent one-electron approximation for electronic eigenvalues $\epsilon_{\vec{k},\mu}$ ($\vec{k}$ is a wave vector; μ is a band index), we can write

$$E_e = E_\Sigma - (V_{ee}{}^{H} + V_{xc}), \quad E_\Sigma = \sum_{\vec{k},\mu} \epsilon_{\vec{k},\mu} f(\vec{k},\mu), \tag{2}$$

where the electron-electron interaction energy double counted in E_Σ is explicitly subtracted off. $V_{ee}{}^{H}$ is the Hartree energy and V_{xc} the exchange and correlation energy. We now write

$$V_0 = V_{cc} - V_{ee}{}^{H} - V_{xc}. \tag{3}$$

V_{xc} is a short-range term and $V_{cc} - V_{ee}{}^{H}$ is much smaller than V_{cc} and has no long-range Coulomb forces if we deal with one atom per unit cell. The cancellation of $V_{cc} - V_{ee}{}^{H}$ is the better the more tightly bound are the atomic orbitals.

Let us denote the contribution $\nabla\nabla V_0$ to the dynamical matrix by D_0. We now consider the contribution of E_Σ to the dynamical matrix. A crucial point of our procedure is that we adopt the nonorthoganal tight-binding scheme (NTB) for the d electrons in TMC. Not only is it a realistic description of the d electrons, it is the most economical and convenient basis for calculating various properties of TMC. Our recent success in calculating the average squared electron-phonon–interaction matrix element[5] for the $4d$ bcc transition metals and alloys further reinforces the conclusions of Friedel[6] and Mott to this effect. In NTB, the Bloch functions are expanded as

$$\psi_{\vec{k},\mu} = N^{-1} \sum_{i,m} \varphi_{im}(\vec{r}) \exp(i\vec{k}\cdot\vec{R}_i) A_{m\mu}(\vec{k}),$$

where m is the orbital index. A satisfies the equation,

$$HA = SAE, \tag{4}$$

with the normalization $A^\dagger SA = 1$. Here E is the diagonal matrix of eigenvalues $\epsilon_{\vec{k},\mu}$, and H and S are the Fourier-transformed tight-binding Hamiltonian and overlap matrices, respectively. It is important to note that the matrix elements $H_{in,jm}$ and $S_{in,jm}$ are regarded here as self-consistent matrix elements including the effects of electron-electron interaction. Since results of self-consistent augmented-plane-wave (APW) band-structure calculations[7] for transition metal are available, a simple way of obtaining these quantities is to fit such a band structure with the NTB scheme.

The contribution to the dynamical matrix from E_Σ can now be written in terms of the variations in $H_{in,jm}$ and $S_{in,jm}$ as the atoms are moved. The contributions will be of two kinds: (i) D_1, from changes in H and S that are second order in the displacements—treated in first-order perturbation theory; and (ii) D_2, from changes in H and S that are first order in the displacements—treated in second-order perturbation theory. It is easy to see that the range of D_1 is about the same as the range of the matrix elements H_{ij} or S_{ij} in the NTB scheme; thus it will be short-ranged for TMC.

The contribution D_2 for a given wave vector $\vec{q} = \vec{k} - \vec{k}'$ is

$$D_2{}^{\alpha\beta}(\vec{q}) = -\sum_{\vec{k},\mu,\vec{k}',\mu'} \frac{g_{\vec{k},\mu;\vec{k}',\mu'}{}^{\alpha *} g_{\vec{k},\mu;\vec{k}',\mu'}{}^{\beta}}{\epsilon_{\vec{k},\mu} - \epsilon_{\vec{k}',\mu'}} (f_{\vec{k}',\mu'} - f_{\vec{k},\mu}), \tag{5}$$

where $g_{\vec{k},\mu;\vec{k}',\mu'}{}^{\alpha}$ is the fully renormalized self-consistent electron-phonon–interaction matrix element (or electron-ion form factor), which we have derived earlier[5]:

$$g_{\vec{k},\mu;\vec{k}',\mu'}{}^{\alpha} = \sum_{m,n} A_{\mu m}{}^{\dagger}(\vec{k}) [\gamma_{mn}{}^{\alpha}(\vec{k}) - \gamma_{mn}{}^{\alpha}(\vec{k}')] A_{n\mu'}(\vec{k}'), \tag{6}$$

with

$$\gamma_{mn}{}^{\alpha}(\vec{k}) = \sum_{\vec{R}_{ij}} (\nabla_\alpha H_{im,jn} - \epsilon_{\vec{k}} \nabla_\alpha S_{im,jn}) \exp(i\vec{k}\cdot\vec{R}_{ij}). \tag{7}$$

The customary method[4] deals with the bare ion-ion dynamical matrix instead of D_0 and then uses the bare electron-ion matrix element instead of g and the fully renormalized susceptibility. The latter quantity is extremely hard to calculate accurately for materials with nonuniform charge densities. Our method avoids this difficulty by grouping terms differently[8]; the *total* dynamical matrix is, of course, identical with the customary one.

The computational advantages of the NTB approach are as follows: (i) The changes in the Hamiltonian due to ion motion are expressed in terms of derivatives of matrix elements taken at discrete lattice points i, j, etc. Thus we do not explicitly require the knowledge of the wave functions and potential gradients at all points in space and yet include all local-field effects. (ii) The effect of variation in screening, exchange, and cor-

relations is included in the terms ∇H_{ij} and ∇S_{ij}, as long as these quantities are determined from self-consistent band-structure calculations at different lattice configurations. (iii) The significant ∇H_{ij} and ∇S_{ij} are confined to a few nearest neighbors. All this makes the calculations economical without introducing any uncontrolled approximations.

Since we expect the term D_2 to cause the long-range oscillatory force fields manifest in the phonon anomalies, we focus our present calculations on D_2. For this we use[5] an NTB band structure with a nine-orbital s-p-d basis fitted to an APW calculation[7] for Nb with an rms error of ~0.15 eV. The NTB matrix elements extend to second neighbors, and the two-center approximation is used. The radial derivatives in the ∇H and ∇S terms are determined from (i) fits to self-consistent APW band-structure calculations at two different lattice constants and (ii) Herman-Skillman atomic wave functions and potentials. The two methods lead to results which agree within ~20%. The short-range term D_0+D_1 is parametrized by four nearest-neighbor (nn) and next-nearest neighbor (nnn) force constants which are fitted such that the diagonalization of $D_0+D_1+D_2$ yields optimum agreement with experimental phonon curves.

With the above procedure and using the rigid-band approximation, we have calculated phonon dispersion for Nb, Mo, and various Nb-Mo alloys. Figure 1 shows the results for Nb, $Nb_{0.25}Mo_{0.75}$, and Mo, together with the experimental results of Powell, Martell, and Woods.[1] The overall quantitative agreement is very good, but more remarkable is the fact that all anomalous features of the phonon dispersion are reproduced. The anomalies in Nb in the longitudinal (L) branches are the dip in the $(\xi, 0, 0)$ direction at $\xi = 0.7$, the deep minima in the (ξ, ξ, ξ) direction at $\xi = 0.7$, and the kink near the point P. In the transverse (T) branches, they are the long-wavelength concavity in the $(\xi, 0, 0)$ and $(\xi, \xi, 0)$ directions and the crossing of the two T branches near the zone boundary in the $(\xi, \xi, 0)$ directions. In Mo, the anomalies are the deep minimum at H with the crossing of L and T in (ξ, ξ, ξ) near H and the soft N_3 mode. In the Nb_x-Mo_{1-x} alloys the anomalies of Nb disappear smoothly with decreasing x, to be replaced by the anomalies of Mo.

We have carefully analyzed our calculation to trace the source of the anomalies, and the nature of the overall spectrum. The most important results with special reference to the $(\xi, 0, 0)$ L branch of Nb are discussed below. The nn and

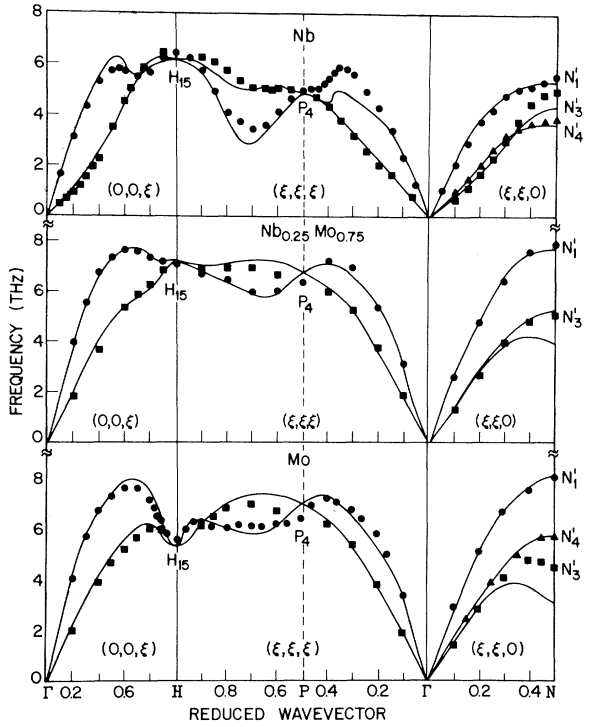

FIG. 1. Calculated phonon dispersion curves for Nb, $Nb_{0.25}Mo_{0.45}$, and Mo. The circles, squares, and triangles are the experimental results of Ref. 1.

nnn force constants representing D_0+D_1 lead to phonon frequencies of about twice the final frequencies. D_0+D_1 vary smoothly increasing by about 20% from Nb to Mo. The contribution of D_2 due to scattering from the dominantly d-like bands to the higher-lying s-p bands has the form of near-neighbor force constants and simply reduces D_0+D_1. The anomalous structure in $D_2(\vec{q})$ is predominantly caused by scattering between d orbitals. Further, variations in ∇H_{ij} elements by (20–30)% or omitting nonorthogonality corrections in g only changes the magnitude of D_2, but not significantly its $\vec{q}$ dependence.

Further analysis has revealed that all the phonon anomalies (except the concavity in the Nb-T branch) are from $D_2^<$, the contribution to D_2 of scattering between states which are within about 0.5 eV of the Fermi surface,[9] as demonstrated for the Nb $(\xi, 0, 0)$ L branch in Fig. 2. However the phonon anomalies are not Fermi-surface anomalies in the Kohn-Overhauser[10] sense. In Fig. 2 this is illustrated by plotting $D_2^<$ with the matrix elements g set at some average constant value (contact approximation).

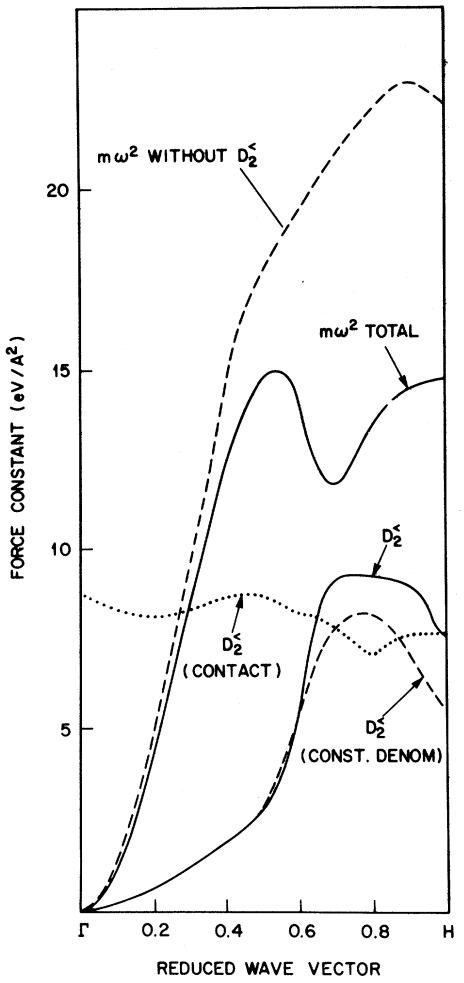

FIG. 2. Analysis of the contribution to the calculated dynamical matrix for the $(\xi,0,0)$ longitudinal branch in Nb. The description of the various curves is given in the text. The aim of this figure is to illustrate that the phonon anomaly arises from the wave-vector dependence of the electron-ion form factor.

The anomalies arise from the $\vec{q}$ dependence of the electron ion form factor g for scattering close to the Fermi surface (F.S.). This is evident in the plot of $D_2^<$ with a constant energy denominator, equal to the inverse density of states, also shown in Fig. 2. We find that even in Mo with a rather favorable Fermi surface for Kohn-Overhauser anomalies near H, the form factors g determine the sharpness of the anomaly. For a physical understanding of these results we note that g can be written approximately as

$$g_{\vec{k},\mu;\vec{k}',\mu'}{}^{\alpha} \sim (v_{\vec{k},\mu}{}^{\alpha} - v_{\vec{k},\mu'}{}^{\alpha}) \sum_m A_{\mu m}^{\dagger}(\vec{k}) A_{\mu' m}(\vec{k}'), \quad (8)$$

where $v_{\vec{k},\mu}{}^{\alpha}$ is the velocity $\partial\epsilon_{\vec{k},\mu}/\partial k^{\alpha}$. The form (8) reflects that the matrix elements are larger when small displacements cause larger changes in electronic energies, and the overlap of initial and final states is larger. Inserting (8) in (5), we conclude that a lattice distortion of wave vector $\vec{q}=\vec{k}-\vec{k}'$ will reduce the energy of a state $(\vec{k},\mu)$ near the F. S. significantly if a state $\epsilon_{\vec{k}',\mu'}$ near the F. S. exists such that $|v_{\vec{k},\mu}{}^{\alpha} - v_{\vec{k}',\mu'}{}^{\alpha}|$ is large. This effect is proportional to $|v_{\vec{k},\mu}{}^{\alpha} - v_{\vec{k}',\mu'}{}^{\alpha}|^2$ while the number of states $\epsilon_{\vec{k},\mu}$ near F. S., given by the density of states, is $\sim |\vec{v}_{\vec{k},\mu}|^{-1}$. Thus for nesting of bands near the F. S., the Kohn-Overhauser theory would predict strong phonon anomalies for small $|v_{\vec{k},\mu}{}^{\alpha}|$ whereas our results show that the anomalies occur for large $|v_{\vec{k},\mu}{}^{\alpha}|$, where α is in the nesting direction. In other words largest phonon anomalies occur because of saddle points in the electronic band structure near the Fermi surface. We have confirmed this qualitative picture by computing D_2 using (8) and have always found maxima at the position of the anomalies.

This last result has general significance. In fact (8) may be used to predict phonon anomalies and instabilities in other materials with knowledge of the band structure alone.

We wish to ahank Dr. E. I. Blount for helpful conversations, and Dr. M. Schlüter and Dr. P. Vashishta for providing some computer programs used in the calculations.

[a]Resident Visitor; on leave from Max-Planck-Institut, Stuttgart, West Germany.

[1]B. M. Powell, P. Martel, and A. D. B. Woods, Phys. Rev. 171, 727 (1968).

[2]H. G. Smith and W. Glaser, Phys. Rev. Lett. 25, 1611 (1970), and 29, 353 (1972).

[3]W. Weber, Phys. Rev. B 8, 5082 (1973); S. K. Sinha and B. H. Harmon, Phys. Rev. Lett. 35, 1515 (1975); M. Gupta and A. J. Freeman, Phys. Rev. Lett. 37, 364 (1976); W. Hanke, J. Hafner, and H. Bilz, Phys. Rev. Lett. 37, 1560 (1976).

[4]See, for instance, L. J. Sham, in *Dynamical Properties of Solids*, edited by G. K. Horton and A. A. Maradudin (North-Holland, Amsterdam, 1974).

[5]C. M. Varma, P. Vashishta, W. Weber, and E. I. Blount, to be published.

[6]See, for instance, J. Friedel, in *The Physics of Metals*, edited by J. M. Ziman (Cambridge Univ. Press, Cambridge, 1969).

[7]J. R. Anderson, D. A. Papaconstantapoulos, J. W. McCaffrey, and J. E. Schirber, Phys. Rev. B 7, 5115 (1973); L. F. Mattheiss, Phys. Rev. B 1, 373 (1970).

[8]This grouping was suggested by W. E. Pickett and B. L. Gyorffy, in *Superconductivity of d- and f-band*

Metals, edited by D. H. Douglass (Plenum, New York and London, 1976), and by C. M. Varma and R. C. Dynes, *ibid.*

[9]We have chosen 0.5 eV somewhat arbitrarily to define $D_2^<$. It is the energy near the F.S., scattering within which leads to over 90% of most of the anomalies.

[10]W. Kohn, Phys. Rev. Lett. 2, 393 (1959); A. W. Overhauser, Phys. Rev. Lett. 4, 415 (1960).

Electrical Conductivity in Doped Polyacetylene

C. K. Chiang, C. R. Fincher, Jr., Y. W. Park, and A. J. Heeger

Department of Physics and Laboratory for Research on the Structure of Matter, University of Pennsylvania, Philadelphia, Pennsylvania 19104

and

H. Shirakawa,[a] E. J. Louis, S. C. Gau, and Alan G. MacDiarmid

Department of Chemistry and Laboratory for Research on the Structure of Matter, University of Pennsylvania, Philadelphia, Pennsylvania 19104

(Received 23 June 1977)

Doped polyacetylene forms a new class of conducting polymers in which the electrical conductivity can be systematically and continuously varied over a range of eleven orders of magnitude. Transport studies and far-infrared transmission measurements imply a metal-to-insulator transition at dopant concentrations near 1%.

We find that films of the semiconducting polymer, polyacetylene, show a dramatic increase in electrical conductivity when doped with controlled amounts of the halogens chlorine, bomine, or iodine, and with arsenic pentafluoride (AsF_5). The concentration dependence in combination with far-infrared transmission data suggests the occurrence of a metal-insulator transition as a function of dopant concentration.

Polyacetylene is one of the simplest linear conjugated polymers with a single-chain structure as shown in Fig. 1. Each carbon is σ bonded to one hydrogen and two neighboring carbon atoms consistent with sp^2 hybridization. The π electrons are therefore available to delocalize into a band. In the idealized situation of a uniform chain, the resulting conduction band would give rise to metallic behavior. However, such a system is unstable with respect to bond alternation, which causes the formation of an energy gap in the electronic spectrum. Studies of π-π^* transitions in short-chain polyenes show that the frequencies do not fall as n^{-2} as expected for a free-electron picture, but appear to saturate at $\Delta E_{(n\ \mathrm{large})}{}^{\pi-\pi^*} \simeq 2.4$ eV.[1] Bond alternation is present in the polymer and would be expected to lead to semiconducting behavior. However, Ovchinnikov[1] has stimmated the bond-alternation energy gap to be too small and attributed the observed value to Coulomb correlation effects, i.e., a Hubbard gap.

In a series of studies Shirakawa and co-workers[2-6] succeeded in synthesizing high-quality polycrystalline films of $(CH)_x$, and developed techniques for controlling the *cis/trans* content.[4,5] These materials are semiconductors[6]; the *trans* isomer is the thermodynamically stable form at room temperature.

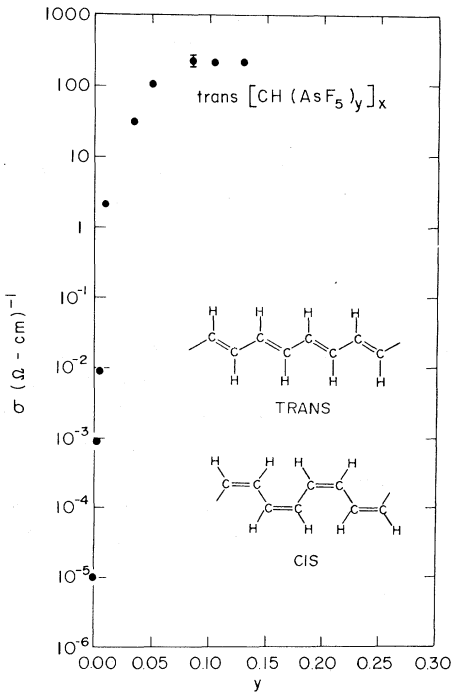

FIG. 1. Electrical conductivity of *trans*-$(CH)_x$ as a function of (AsF_5) dopant concentration. The *trans* and *cis* polymer structures are shown in the inset.